Mixture of Balanced Information Bottlenecks for Long-Tailed Visual Recognition

Anonymous authors
Paper under double-blind review

Abstract

Deep neural networks (DNNs) have achieved significant success in various applications with large-scale and balanced data. However, data in real-world visual recognition are usually long-tailed, bringing challenges to efficient training and deployment of DNNs. Information bottleneck (IB) is an elegant approach for representation learning. In this paper, we propose a *balanced information bottleneck* (BIB) approach, in which loss function re-balancing and self-distillation techniques are integrated into the original IB network. BIB is thus capable of learning a sufficient representation with essential label-related information fully preserved for long-tailed visual recognition. To further enhance the representation learning capability, we also propose a novel structure of *mixture* of multiple *balanced information bottlenecks* (MBIB), where different BIBs are responsible for combining knowledge from different network layers. MBIB facilitates an end-to-end learning strategy that trains representation and classification simultaneously from an information theory perspective. We conduct experiments on commonly used long-tailed datasets, including CIFAR100-LT, ImageNet-LT, and iNaturalist 2018. Both BIB and MBIB reach state-of-the-art performance for long-tailed visual recognition.

1 Introduction

With the emergence of ImageNet, COCO, and other datasets, deep neural networks (DNNs) have achieved great success in various computer vision tasks such as image classification, object detection, and image segmentation. The success of deep learning is largely due to the large-scale and balanced data in these tasks. However, real-world data are usually long-tailed Buda et al. (2018), which means that a few classes (head classes) occupy most instances in the data, while most classes (tail classes) occupy only a few instances. When using standard training methods (using cross entropy as the loss function and instance balanced sampling) to train a model on a long-tailed training set, the model usually performs well for the head classes but poorly for the tail classes, which brings a great challenge to the training and deployment of DNNs Buda et al. (2018).

Recently, many methods have been proposed to solve the problem of imbalanced data distribution. Among these methods, re-sampling and loss function re-balancing are the two most commonly used techniques. Re-sampling makes an imbalanced dataset balanced by over-sampling or under-sampling Buda et al. (2018); Ando & Huang (2017). Re-balancing methods include re-weighting Buda et al. (2018) and the logits adjustment Ren et al. (2020). Kang et al. (2019) found that although the classification performance of a model trained by standard methods is worse than that of re-balancing methods, the obtained feature space is better. They proposed to decouple the training process into two stages: learning representation and learning classifier. The decoupling training method leads to good results Peifeng et al. (2023); Zhou et al. (2023); Zhang et al. (2021). Zhong et al. (2021) showed that partial network parameters obtained in the learning representation stage, such as parameters of Batch Normalization (BN), are not suitable for the second stage of learning classifier directly, which suggests that learning representation and learning classifier should not be regarded as two completely independent stages. Mixture-of-Experts (MoE) techniques involve the training of multiple neural networks, each specializing in handling distinct segments of a long-tailed dataset. BBN Wang et al. (2020), RIDE Zhou et al. (2020b) and SADE Zhang et al. (2022) serve as representations of MoE

methods. However, the enhanced capabilities of MoE come at the cost of increased computational loads. Recently, Laurent et al. (2022) highlighted that, for long-tailed visual recognition, the key is not just the classification rule but the ability to learn and identify correct features.

The Information Bottleneck (IB) is an elegant approach for representation learning. It originates from the rate-distortion theory Tishby (1999); Tishby & Zaslavsky (2015), and has made extraordinary progress in many tasks, such as image classification Alemi et al. (2017), image segmentation Luo et al. (2019), multi-view learning Wang et al. (2021b), reinforcement learning Goyal et al. (2019) and so on. IB rethinks what a "good" representation is: for a given task, the best representation should contain sufficient and minimal amount of information. In the IB theory, sufficiency is achieved by maximizing the mutual information between the representation z and the label y, and minimality is achieved by minimizing the mutual information between the input x and the representation z. By introducing a Lagrange multiplier β, the IB method can be optimized by minimizing

$$R_{IB} = -I(z; y) + \beta I(x; z), \tag{1}$$

where $I(a; b)$ represents the mutual information between a and b. IB provides a new learning paradigm that naturally avoids over-fitting and enhances model robustness. To optimize the IB objective in problems involving high-dimensional variables, variants such as VIB Alemi et al. (2017), Drop-IB Kim et al. (2021), and Nonlinear-IB Kolchinsky et al. (2019) are proposed. VIB is the first to indirectly optimize the variational upper bound of IB, and has become one of the most widely used IB variants for its simplicity and effectiveness.

Although IB has made a lot of progress on balanced datasets, $I(z; y)$ is still affected by label distribution when applied to long-tailed datasets. This limitation arises from the scarcity of tail class samples, making it difficult for DNNs to learn a sufficient representation z. Besides, the mutual information is difficult to estimate in DNNs. To solve these problems, we propose a novel *balanced* information bottleneck (BIB) method in this study. We use the loss function re-balancing technique to alleviate challenges posed by label distribution. Concurrently, we implicitly optimize the information bottleneck objective by self-distillation to reserve as much information related to labels as possible in the process of information flow. To further enhance the representation learning ability, we introduce a novel framework of a mixture of multiple *balanced* information bottlenecks (MBIB). MBIB is the first network to leverage *multiple* balanced information bottlenecks, each responsible for extracting knowledge from different network layers. By optimizing multiple IB objectives simultaneously, MBIB ensures a comprehensive and effective representation learning process, leading to improved performance. We conduct experiments on benchmark datasets, including CIFAR100-LT, ImageNet-LT, and iNaturalist 2018.

The contributions of this study are summarized as follows:

1) Firstly, we propose a novel *balanced* information bottleneck (BIB) method to handle long-tailed data for real-word visual recognition.
2) Secondly, to the best of our knowledge, we propose the first network with a mixture of *multiple* balanced information bottleneck (MBIB), optimizing diverse IB objectives simultaneously to effectively learn representation and classifier in an end-to-end fashion.
3) Finally, our methods achieve state-of-the-art performance according to the average classification accuracy across multiple benchmark datasets.

2 Related Work

2.1 Long-Tailed Visual Recognition

Re-sampling and loss function re-balancing are the most widely studied approaches in imbalanced classification. Re-sampling aims to construct a balanced training set, including over-sampling and under-sampling. Due to the low diversity of tail classes, over-sampling often results in models over-fitting tail classes. Under-sampling discards part of samples in head classes, which damages the diversity of head classes and decreases model generalization performance. Kang et al. (2019) proposed a progressive sampling algorithm combining over- and under-sampling to transition the distribution from an imbalanced distribution to a balanced distribution. However, the problem of re-sampling still exists.

Loss function re-balancing gives different weights to different classes or instances to re-balance the model at the level of the loss function. This strategy mainly includes re-weighting Cui et al. (2019); Byrd & Lipton (2019) and logits adjustment Ren et al. (2020); Menon et al. (2021). Cui et al. (2019) proposed re-weighting the loss function with the number of effective samples. Lin et al. (2020) suggested that the model should pay more attention to hard samples by giving hard samples a large weight. On the other hand, Ren et al. (2020) and Menon et al. (2021) adjusted logits to make gradients more balanced during training. Kang et al. (2019) found that although re-balancing and re-sampling can improve the performance of imbalanced classification, they result in worse representation. Kang et al. (2019) proposed to decouple the training process into two stages. The first stage uses standard training methods to learn a good representation. In the second stage, strategies such as re-sampling, re-weighting and so on are used to fine-tune the classifier to learn a good classifier. The decoupling training approach provides a new training paradigm for long-tailed recognition. Many studies have focused on how to obtain better representation Kang et al. (2021); Liu et al. (2021); Zhong et al. (2022) or learn a better classifier Wang et al. (2021d;a); Zhong et al. (2021). MoE methods also have achieved a great success by effectively combining the knowledge from multiple experts. BBN Zhou et al. (2020b) introduces a two-branches network to address long-tailed recognition. RIDE Wang et al. (2020) trains multiple experts with the softmax loss respectively and enforces a KL-divergence based loss to enhance the diversity among various experts. SADE Zhang et al. (2022) pioneers a novel spectrum-spanned multi-expert framework and introduces an innovative expert training scheme. Distillation strategy like DiVE He et al. (2021) and contrastive learnig like PaCo Cui et al. (2021) have also achieved successes.

2.2 Information Bottleneck

IB divides the model into two parts: an encoder and a decoder. The encoder codes a random variable x into a random variable z, and the decoder decodes the random variable z into a random variable y. IB assumes that variables x, z, y follow a Markov chain $y \leftrightarrow x \leftrightarrow z$, and z is the bottleneck of information flow. IB expects z to retain information from x to y as much as possible while forgetting information unrelated to y. It means that for a given task, z is the best representation in the perspective of rate-distortion. However, despite the beauty of the IB theory, the calculation of the mutual information in IB is complicated, especially in deep learning Slonim (2006). To tackle this problem, Variational Information Bottleneck (VIB) Alemi et al. (2017) optimizes the IB objective by using its upper bound. According to VIB, $-I(z;y)$ and $I(x;z)$ are bounded as

$$\begin{aligned} -I(z;y) &\leq E_{p(z,y)} - \log q(y|z) = L_{CE}(z,y), \\ I(x;z) &\leq E_{p(x,z)} \log p(z|x) - E_{p(z)} \log r(z) \\ &= E_{p_{data}(x)}[KL(q(z|x)||r(z))], \end{aligned} \tag{2}$$

where $q(y|z)$, $q(z|x)$, $r(z)$ are the variational approximations to $p(y|z)$, $p(z|x)$, $p(z)$, respectively. VIB is widely used for its simplicity and effectiveness. However, IB is essentially a compromise between representation and classification, and obtaining an optimal compromise point is difficult. To avoid this compromise, Tian et al. (2021) proposed a method to implicitly optimize the information bottleneck objective through self-distillation.

3 Method

3.1 Preliminaries

Let $D = \{(x_i, y_i)\}_{i=1}^{N}$ be a training set, where y_i is the label for data x_i and K is the number of classes. Without loss of generality, let $n_1 > n_2 > \cdots > n_K$, where n_i is the number of training samples for class i, hence the total number of training samples is $N = \sum_{i=1}^{K} n_i$. Unlike the long-tailed distribution of the training set, the test set follows a uniform distribution, ensuring an equal number of samples across all classes for a balanced evaluation of the model's performance in each class.

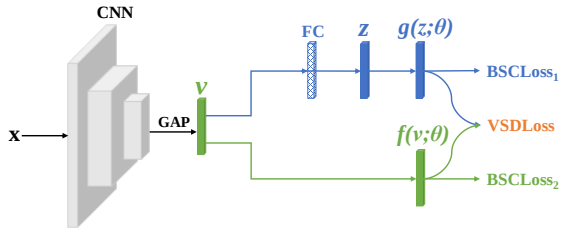

Figure 1: The network structure of BIB. FC means the Fully Connected layer and GAP means Global Average Pooling, $f(v;\theta)$ and $g(z;\theta)$ are classifiers. BSCLoss means the balanced softmax cross entropy loss ($Loss_1$ and $Loss_2$), and VSDloss means variational self-distillation loss ($Loss_3$). The output is the mean of the outputs from $f(v;\theta)$ and $g(z;\theta)$.

3.2 Balanced Information Bottleneck (BIB)

The information bottleneck theory aims to obtain a sufficient and minimal representation of the input, in the sense of effectively characterizing the output. Let v be an observation of the input x extracted from an encoder such as a CNN, and z be a representation encoded from v by a fully connected layer, as shown in Figure 1. Considering CNNs' powerful feature extraction capability, it's reasonable to assume that v may retain all label information from the input x. Therefore, our problem is translated into how to find a representation z that preserves the sufficient and minimal information of the observation v to the label y. To address this, we decompose $I(v;z)$ to two terms Tian et al. (2021):

$$I(v;z) = I(z;y) + I(v;z|y), \tag{3}$$

where the first term represents the information in z that is related to the label, and the second term represents information that is not related to the label. To optimize the IB objective, we should maximize $I(z;y)$ while minimizing $I(v;z|y)$. Minimizing $I(v;z|y)$ is equivalent to minimizing $|I(v;y) - I(z;y)|$ Tian et al. (2021). Therefore, we can decompose the objective into three sub-optimization objectives: maximizing $I(v;y)$, maximizing $I(z;y)$ and forcing $I(z;y)$ to approximate $I(v;y)$.

To handle long-tailed data, we propose a *balanced information bottleneck* (BIB), in which loss function re-balancing and self-distillation class weighting techniques are integrated into the original IB network. We start with maximizing $I(v;y)$ and $I(z;y)$. According to VIB Alemi et al. (2017), $-I(v;y)$ and $-I(z;y)$ are bounded as $E_{p(v,y)} - \log q(y|v)$ and $E_{p(z,y)} - \log q(y|z)$. For a long-tailed dataset, we apply a re-balance technique over $I(v;y)$:

$$p_s(y_i|v) \approx q_s(y_i|v) = \frac{n_i e^{f_i(v;\theta)}}{\sum_{j=1}^{K} n_j e^{f_j(v;\theta)}}, \tag{4}$$

where the subscript s represents the training set distribution, $f(v;\theta)$ represents the classifier following v. The proof can be found in Appendix A. The loss corresponding to maximizing $I(v;y)$ becomes:

$$Loss_1 = E_{p(v,y)} - \log q_s(y|v). \tag{5}$$

Similarly, to maximize $I(z;y)$, we get the loss as:

$$Loss_2 = E_{p(z,y)} - \log q_s(y|z). \tag{6}$$

$Loss_1$ and $Loss_2$ are cross entropy losses. We introduce a classes weighting factor inversely proportional to the label frequency to strengthen the learning of the minority class and re-balance the losses better. The weighting factor is:

$$w_i = \frac{K \cdot (1/d_i)^m}{\sum_{i=1}^{K} (1/d_i)^m}, \tag{7}$$

where d_i is the i-th class frequency of the training dataset, and m is a hyperparameter. Therefore, $Loss_1$ and $Loss_2$ are regarded as balanced softmax cross entropy losses (BSCLoss).

Then, to force $I(z;y)$ to approximate $I(v;y)$, we only need to ensure that $H(y|v)$ approximates $H(y|z)$. Tian et al. (2021) proved that making $q(y|v)$ approximate $q(y|z)$, i.e., minimizing the KL-divergence between $q(y|z)$ and $q(y|v)$, can effectively make $H(y|v)$ approximate $H(y|z)$. Therefore, our third loss is to minimize the $D_{KL}[q(y|v)||q(y|z)]$:

$$\begin{aligned} Loss_3 &= E_{q(v|x)}[D_{KL}[q(y|v)||q(y|z)]] \\ &= E_{q(v|x)}[E_{q(z|v)}[q(y|v)[\log q(y|v) - \log q(y|z)]]] \\ &= E_{q(v|x)}[E_{q(z|v)}[-H(y|v) - q(y|v)\log q(y|z)]]. \end{aligned} \tag{8}$$

Note that this is like the method of self-distillation. To stabilize the optimization, we don't optimize $q(y|v)$; instead, we detach it from the backward propagation process. We call $Loss_3$ the variational self-distillation loss (VSDLoss). Furthermore, to mitigate the effect of the long-tailed distribution, we use class-dependent self-distillation temperatures: $q(y_i|v) = \frac{e^{f_i(v;\theta)/T_i}}{\sum_{j=1}^{K} e^{f_j(v;\theta)/T_j}}$ and $q(y_i|z) = \frac{e^{g_i(z;\theta)/T_i}}{\sum_{j=1}^{K} e^{g_j z;\theta)/T_j}}$, where $T_i = (\frac{n_{max}}{n_i})^{\gamma}$, γ is a hyperparameter, $g(v;\theta)$ represents the classifier following v.

The overall loss is given by

$$Loss_{BIB(v,z)} = Loss_1 + Loss_2 + \beta \cdot Loss_3, \tag{9}$$

where β is a hyperparameter. To sum up, $Loss_1$ and $Loss_2$ are balanced cross entropy losses (BSCLoss) to maximize $I(v;y)$ and $I(z;y)$. $Loss_3$ is the variational self-distillation loss (VSDLoss) to force $I(z;y)$ to approximate $I(v;y)$. Therefore, we can optimize the IB objective implicitly by minimizing $Loss_{BIB(v,z)}$.

3.3 Mixture of Balanced Information Bottleneck (MBIB)

In BIB, v serves as the observation derived from CNN on the input x, and it is assumed that $I(v;y) = I(x;y)$, implying that v retains all mutual information between x and the label y. However, this assumption encounters limitations due to the inherent data processing inequality Cover & Thomas (1991) in the information processing chain. Specifically, during the feature extraction process of a CNN network with three parts (CNN_1, CNN_2 and CNN_3), as illustrated in Figure 2, there is a diminishing trend in mutual information:

$$I(v_3;y) \leq I(v_2;y) \leq I(v_1;y). \tag{10}$$

Here, v_1 and v_2 represent intermediate observations from the partial CNNs, and v_3 is the observation of the entire CNN on x (i.e., v in BIB in Section 3.2). Hence, the assumption that $I(v;y) = I(x;y)$ in BIB doesn't always hold; instead, $I(v;y) \leq I(x;y)$ due to information loss. Therefore, v (v_3 in Figure 2) is not a sufficient observation containing all mutual information between x and the label y. Consequently, solely applying BIB between v and z may not fully utilize the label-related information.

One promising model enhancement strategy is leveraging information retained in v_1 and v_2, given that they contain more mutual information with y than v_3. By applying BIB between v_1 and z ($BIB(v_1, z)$), as well as between v_2 and z ($BIB(v_2, z)$), we are able to conserve a more substantial portion of mutual information relating to label y in v_1 and v_2, thereby making feature z a sufficient and comprehensive representation of v_1, v_2, and v_3 simultaneously.

Hence, we propose a novel network structure, which consists of the *mixture* of *multiple balanced information bottleneck* (i.e., MBIB), as shown in Figure 2. MBIB is a network capable of simultaneously optimizing diverse information bottleneck. The overall loss function is:

$$Loss_{MBIB} = a \cdot Loss_{BIB(v_1,z)} + b \cdot Loss_{BIB(v_2,z)} + Loss_{BIB(v_3,z)}, \tag{11}$$

where a and b are hyperparameters to adjust the proportions of different BIBs. Specifically, when $a = 0$ and $b = 0$, MBIB degrades to the BIB proposed in Section 3.2. As the values of a and b increase, the model

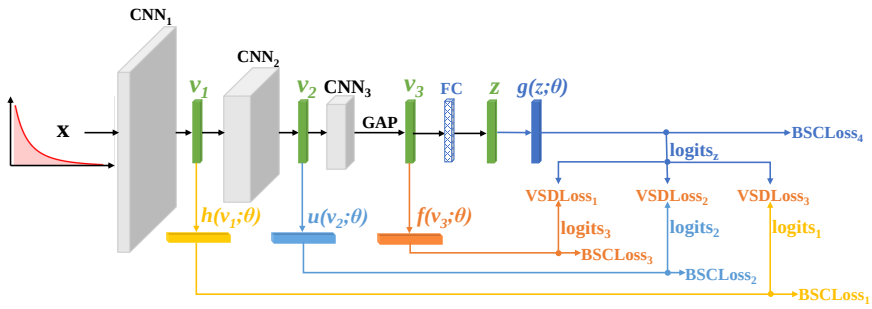

Figure 2: The network structure of MBIB. CNN_1, CNN_2 and CNN_3 are different parts of the CNN network. FC means the Fully Connected layer, and GAP means Global Average Pooling. $h(v_1;\theta)$, $u(v_2;\theta)$, $f(v_3;\theta)$ and $g(z;\theta)$ are classifiers. The output is the mean of the outputs from $f(v_3;\theta)$ and $g(z;\theta)$.

emphasizes information from v_1 and v_2 more. Each $Loss_{BIB}$ is composed of three losses as below:

$$Loss_{BIB} = BSCLoss_1 + BSCLoss_2 + \beta \cdot VSDLoss, \tag{12}$$

where there are two balanced cross entropy losses and one variational self-distillation loss.

From the perspective of self-distillation, we can further explore the effectiveness of MBIB. VSDLosses in Eqs. equation 9 and equation 12 facilitate self-distillation processes among layers at different depths and the output layer. For example, the VSDLoss in $BIB(v_1, z)$ is optimized in the following form:

$$minVSDLoss_{BIB(v_1,z)} \Leftrightarrow minE_{q(v_1|x)}[D_{KL}[q(y|v_1)||q(y|z)]]. \tag{13}$$

To optimize this objective, we minimize the KL-divergence between $q(y|z)$ and $q(y|v_1)$, thereby performing distillation between v_1 and z. This process effectively integrates knowledge from v_1 and z.

Previous studies Jin et al. (2023) have underscored that shallow parts of the deep model are able to perform better on certain tail classes, and layers of different depths excel at recognizing different classes in long-tailed data. This suggests that fusing knowledge from shallow and deep layers can better fit the long-tailed data, and VSDLosses achieve this through self-distillation.

Therefore, MBIB enables a more comprehensive output that integrates the knowledge of different shallow layers. At the same time, this approach allows shallow layers to learn from deeper ones. Consequently, this strategy can enhance the representation learning capability of the network by integrating knowledge form different depths.

4 Experiments

4.1 Datasets and Setup

Long-Tailed CIFAR-100. CIFAR-100 includes 60K images, of which 50K images are for training and 10K for verification. There are 100 classes in total. We use the same long-tailed version of the CIFAR-100 dataset as in Cao et al. (2019) for a fair comparison. The imbalance degree of the dataset is controlled by the Imbalanced Factor ($IF = N_{\max}/N_{\min}$, where $N_{\max}$ represents the highest frequency and $N_{\min}$ represents the lowest frequency). We conduct experiments on CIFAR-100-LT with IF of 100, 50, and 10.

ImageNet-LT. ImageNet-LT is a subset of long-tailed distribution sampled from ImageNet through Pareto distribution. The ImageNet-LT training set contains 115.8K images, and a total of 1000 classes. The highest frequency is 1280, and the lowest frequency is 5. There are 20 images of each class in the validation set, and 50 images in each class of the test set.

iNaturalist 2018. iNaturalist 2018 is a large-scale, long-tailed fine-grained dataset. iNaturalist 2018 includes 437.5K images and 8142 classes in total, with 1000 samples for the class with the highest frequency and 2 samples for the class with the lowest frequency.

Table 1: Top-1 accuracy(%) of ResNet32 on CIFAR-100-LT with 200 epochs. Data in bold is the overall accuracy of our methods, while underlined data indicates overall performances superior to ours. This formatting is consistent in other tables.

Method	Imbalanced Factor		
	100	50	10
One-Stage			
CE	38.3	43.9	55.7
Focal Loss	38.4	44.3	55.8
LDAM-DRW	42.0	46.6	58.7
BBN	42.6	47.0	59.1
CDT	44.3	-	58.9
BSCE	42.7	47.2	58.5
BIB(Ours)	**44.9**	**49.8**	**60.4**
MBIB(Ours)	**47.5**	**51.2**	**60.9**
Two-Stage			
cRT	41.2	46.8	57.9
τ-norm	41.1	46.7	57.1
KCL	42.8	46.3	57.6
TSC	43.8	47.4	59.0
SSP	43.4	47.1	58.9
MoE			
BBN	42.6	47.0	59.1
RIDE(2E)	47.0	-	-
RIDE(3E)	<u>48.0</u>	-	-
SADE	<u>49.8</u>	<u>53.9</u>	<u>63.6</u>
Others			
DiVE	45.4	51.1	<u>62.0</u>

According to the setting in Liu et al. (2019), we divide the dataset into three subsets according to the number of samples: Many shot (more than 100 samples), Medium shot (between 20 and 100 samples), and Few shot (less than 20 samples).

4.2 Implementation Details

Training details on CIFAR-100-LT. For CIFAR-100-LT, we process samples in the same way as in Cao et al. (2019); Zhou et al. (2020a). We use ResNet32 as the backbone network. To keep consistent with the previous settings Cao et al. (2019), we use the SGD optimizer with a momentum of 0.9 and weight decay of 0.0003. We train 200 epochs for each model. The initial learning rate is set to 0.1, and the first five epochs use the linear warm-up. The learning rate decays by 0.01 at 160th and 180th epoch. The batch size of all experiments is set to 128.

Training details on ImageNet-LT. For ImageNet-LT, we report the results of two backbone networks: ResNet10 and ResNeXt50. We train 90 epochs for all models, using the SGD optimizer with a momentum of 0.9 and weight decay of 0.0005. For ResNet10, we use a cosine learning rate schedule decaying from 0.05 to 0 with batch size of 128. For ResNeXt50, we use a cosine learning rate schedule decaying from 0.025 to 0 with batch size of 64.

Training details on iNaturalist 2018. For the iNaturalist 2018, we use ResNet50 as the backbone network. The model trained 90 or 200 epochs using the SGD optimizer with a momentum of 0.9 and weight decay of 0.0001. The batch size is set to 64, and we use a cosine learning rate schedule decaying from 0.025 to 0.

For the setting of hyperparameters, we take β in $\{0, 1, 2, 3, 4, 5\}$ according to different datasets. For all of the datasets, we use $a = 0.1$, $b = 0.3$ and $m = 0.1$. For CIFAR100-LT, we use $\gamma = 0$, and for ImageNet-LT and iNaturalist 2018, we use $\gamma = 0.5$. To make the results more robust, we use the mean of $f(v; \theta)$ and $g(z; \theta)$ as the final result of the test sample.

4.3 Main Results

Baseline. We compared four mainstream approaches, including one-stage, two-stage, MoE and other approaches such as distillation and contrastive learning. The one-stage approach includes Focal loss Lin et al. (2020), LDAM Cao et al. (2019), CDT Ye et al. (2020), BSCE Ren et al. (2020), weight balancingAlshammari et al. (2022), RBLPeifeng et al. (2023), etc. The two-stage approach includes cRT Kang et al. (2019), τ-norm Kang et al. (2019), KCL Kang et al. (2021), TSC Li et al. (2021), SSP Yang & Xu (2020), WCDASHan (2023), CC-SAMZhou et al. (2023), etc. The MoE approach includes BBNZhou et al. (2020b), RIDEWang et al. (2020), SADEZhang et al. (2022). The distillation approach is DiVEHe et al. (2021). The contrastive learning method is PaCoCui et al. (2021). Especially, if only the results of the v are concerned, BIB degenerates to BSCE.

CIFAR-100-LT. Table 1 compares BIB and MBIB with baseline methods on CIFAR-100-LT. As the results show, BIB achieves improvements on all imbalanced factors. MBIB is higher than most of the methods and even outperforms some MoE models. Although some MoE methods outperform MBIB, they incur much larger computational costs than our methods.

ImageNet-LT. Table 2 compares BIB and MBIB with baseline methods on ImageNet-LT. We conduct experiments on two backbones networks: ResNet10 and ResNeXt50. The results of RIDE, SADE and PaCo are from Zhang et al. (2023). The experimental results show that BIB and MBIB can achieve consistent performance improvement on both small and large neural networks. The overall accuracy of MBIB is higher than all of the baseline methods except SADE.

iNaturalist 2018. Table 3 compares BIB with baseline methods on iNaturalist 2018. Notably, MBIB achieves the best performance for 200 training epochs among all of the baseline methods including MoE models.

4.4 Ablation Study

How the value of β affects our methods? β is a hyperparameter in the loss function, which affects the degree of information compression by the network. Figure 3 shows the impact of different β on the overall accuracy of the CIFAR100-LT dataset. The results show that the optimal β may be different for different imbalanced factors and different methods, and we can make more fine adjustments if necessary. However, we think this may not be necessary, because simple search in $\{0, 1, 2, 3, 4, 5\}$ can already obtain satisfactory results.

How the the value of a and b affects our methods? a and b are hyperparameters that adjust the proportions of different BIB components within the MBIB framework. Figure 4 shows the heatmap of accuracy on the CIFAR100-LT dataset with respect to different a and b. The results show that the values of a and b significantly influence the overall accuracy. Similar to the β, we can fine-tune a and b to get the models having better performances.

How the the quantity of observation v affects our methods? We utilize three observation v in our methods. Ablations on a and b show that when a or b is zero, 3-MBIB (three-observation MBIB) degenerates to 2-MBIB and accuracy often lowers. We also investigated 4-MBIB, with results shown in Table 4. We found the quantity of observation v affects MBIB's performance, improving with more v. However, once v exceeds 3, the performance improvement diminishes as the v quantity continues to increase. We attribute this to the fact that 3-MBIB has fully utilized the useful information in intermediate observations, thereby limiting the additional information gained by further increasing v, resulting in a smaller improvement for 4-MBIB.

Table 2: Top-1 accuracy(%) of ResNet10 and ResNeXt50 on ImageNet-LT with 90 epochs. A ‡ or † indicates training extended to 180 or 200 epochs.

Method	ResNet10/ResNext50			
	Many	Medium	Few	All
One-Stage				
CE	57.0/65.9	25.7/37.5	3.5/7.7	34.8/44.4
Focal Loss	36.4/64.3	29.9/37.1	16.0/8.2	30.5/43.7
LDAM-DRS	-/63.7	-/47.6	-/30.0	36.0/51.4
LADE	-/62.3	-/49.3	-/31.2	-/51.9
BSCE	53.4/62.2	38.5/48.8	17.0/29.7	41.3/51.4
weight balancing†	-/62.0	-/49.7	-/41.0	-/53.3
RBL†	-/64.8	-/49.6	-/34.2	-/53.3
BIB(Ours)	54.7/64.7	40.0/51.2	21.7/32.7	**43.2**/**53.9**
MBIB(Ours)	56.4/67.0	41.8/52.8	23.2/33.5	**44.9**/**55.7**
Two-Stage				
cRT	-/61.8	-/46.2	-/27.4	41.8/49.6
τ-norm	-/59.1	-/46.9	-/30.7	40.6/49.4
DisAlign	-/61.5	-/50.7	-/33.1	-/52.6
WCDAS	53.8/-	41.7/-	25.3/-	44.1/-
CC-SAM	-/63.1	-/53.4	-/41.4	-/55.4
SRepr‡	-/-	-/-	-/-	-/54.6
MoE				
BBN	-/40.0	-/43.3	-/40.8	-/41.2
RIDE(3E)	-/66.9	-/52.3	-/34.5	44.3/55.5
SADE	-/65.3	-/55.2	-/42.0	-/57.3
Others				
DiVE	-/64.1	-/50.4	-/31.5	-/53.1
PaCo	-/59.7	-/51.7	-/36.6	-/52.7

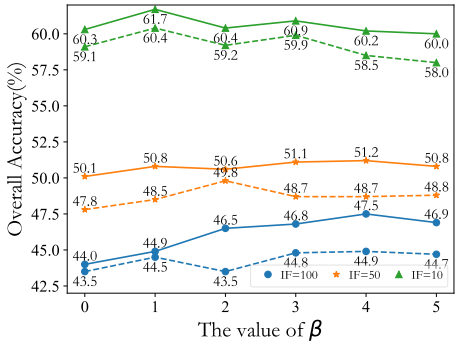

Figure 3: The impact of different β on the overall accuracy of CIFAR-100-LT (we fixed $a = 0.1$ and $b = 0.3$). The solid lines show the results of MBIB and the dashed lines correspond to BIB.

Due to the page limit, the impact of different parts of BIB, as well as comparisons between BIB and BSCE are provided in Appendix B and C.

4.5 Analysis of the Posterior Probability Distribution

Ideally, the mean positive posterior probability of per class should be equal to 1:

$$\overline{q}(y_i|x) = \frac{1}{n_i}\sum_{j=1}^{n_i} q(y_i|x_j) = 1. \tag{14}$$

Table 3: Top-1 accuracy(%) of ResNet50 on iNaturalist 2018.

Method	Epoch	Many	Medium	Few	All
One-Stage					
CE	90/200	72.2/75.7	63.0/66.9	57.2/61.7	61.7/65.8
ResLT Cui et al. (2022)	200	68.5	69.9	70.4	70.2
LADE Hong et al. (2021)	200	-	-	-	70.0
BSCE Ren et al. (2020)	90/200	67.2/69.6	66.5/69.8	67.4/69.7	66.9/69.8
weight balancing Alshammari et al. (2022)	200	71.0	70.3	69.4	70.0
BIB(Ours)	90/200	70.9/73.9	69.9/72.9	69.6/72.1	**69.9/72.7**
MBIB(Ours)	90/200	70.7/72.6	70.6/73.6	70.2/73.1	**70.4/73.3**
Two-Stage					
cRT Kang et al. (2019)	90/200+10	69.0/73.2	66.0/68.8	63.2/66.1	65.2/68.2
τ-norm Kang et al. (2019)	90/200+10	65.6/71.1	65.3/68.9	65.9/69.3	65.6/69.3
KCL Kang et al. (2021)	200+30	-	-	-	68.6
TSC Li et al. (2021)	400+30	72.6	70.6	67.8	69.7
DisAlign Zhang et al. (2021)	90/200+30	64.1/69.0	68.5/71.1	67.9/70.2	67.8/70.6
WCDAS Han (2023)	200+30	75.5	72.3	69.8	71.8
CC-SAM Zhou et al. (2023)	200+30	65.4	70.9	72.2	70.9
SRepr Nam et al. (2023)	200+20	-	-	-	70.8
MoE					
BBN Zhou et al. (2020b)	90/180	49.4/-	70.8/-	65.3/-	66.3/69.6
RIDE(4E) Wang et al. (2020)	100/200	70.9/70.5	72.4/73.7	73.1/73.3	<u>72.6</u>/73.2
SADE Zhang et al. (2022)	200+5	74.5	72.5	73.0	72.9
Others					
DiVE He et al. (2021)	90/200	-/-	-/-	-/-	69.1/71.7
PaCo Cui et al. (2021)	200	68.5	72.0	71.8	71.6

Table 4: Accuracy of MBIB with different quantities of observation v. We set $a = 0$ in 2-MBIB and $a = 0.3, b = 0.3$ in the others. 4-MBIB(x) denotes the introduction of $BIB(x, z)$ to 3-MBIB.

Quantity of v	2-MBIB	3-MBIB	4-MBIB(x)	4-MBIB
Accuracy(%)	45.2	46.6	46.8	46.9

This means that the closer $\overline{q}(y_i|x)$ is to 1, the better. The experiment results reveal BIB's superiority in most classes compared to BSCE and MBIB behaves better than BIB in the tail classes. The detailed results and analysis are shown in Appendix D.

4.6 Analysis of the Learned Representation

A good representation should have the following characteristics: the representations of the same class are very close, and the representations between different classes are far away Wang et al. (2021c). We can evaluate the quality of the representation by the mean of the average intra-class distance (D_{Intra}), the mean

Table 5: The value of ρ of different methods on the CIFAR-100-LT (IF=100) testing set.

Metric	Methods	Many	Medium	Few	All
ρ	BSCE	1.26	1.30	1.48	1.34
	BSCE_MLP	0.85	0.98	1.29	0.99
	BIB_v	0.94	1.06	1.37	1.06
	BIB_z	0.80	0.91	1.15	0.91
	MBIB_v	1.01	1.04	1.31	1.09
	MBIB_z	**0.78**	**0.86**	**1.02**	**0.86**

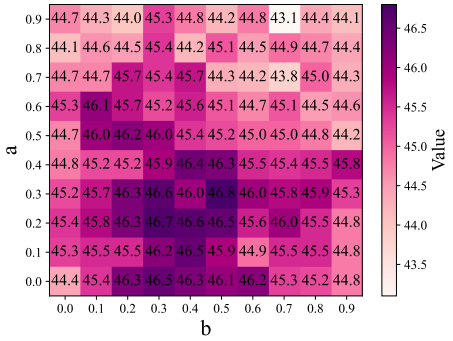

Figure 4: The impact of different a and b on the overall MBIB accuracy of CIFAR-100-LT (we fixed $\beta = 5$).

inter-class distance (D_{Inter}), and the ratio (ρ) between them. D_{Intra}, D_{Inter} and ρ are calculated as follows:

$$D_{Intra} = \frac{1}{K}\sum_{i=1}^{K}\frac{1}{|R_i|^2}\sum_{r_j,r_k\in R_i}\parallel r_j - r_k\parallel_2, \tag{15}$$

$$D_{Inter} = \frac{1}{K(K-1)}\sum_{i=1}^{K}\sum_{j=1,j\neq i}^{K}\parallel c_i - c_j\parallel_2, \tag{16}$$

$$\rho = \frac{D_{Intra}}{D_{Inter}}, \tag{17}$$

where R_i is the representation set of class i, and c_i is the class center of class i, i.e. $c_i = \frac{1}{|R_i|}\sum_{r_j\in R_i} r_j$. The better the representation, the smaller the value of ρ.

Table 5 compares ρ obtained by different methods on the testing set. The value of ρ obtained by BIB and MBIB is smaller than that of BSCE and BSCE_MLP (BSCE_MLP indicates that the network structure is the same as branch z in BSDIB, and the loss function is BSCE). In addition, We visualize the representation of the test set obtained by different models using t-SNE van der Maaten & Hinton (2008). The visualization and its analysis are shown in Appendix E.

Table 6: Efficiency comparisons (test on size $3 \times 640 \times 640$)

Method	MBIB	SADE	RIDE(4E)
Params(k)	**486.02**	783.86	1018.00
FLOPs(G)	**27.93**	40.69	50.98

4.7 The efficiency compared with MoE

MoE methods are often the state-of-the-art approaches in long-tailed recognition. Although they can achieve higher accuracy on some datasets compared to our methods, they always demand much larger computational resources. Therefore, MoE methods are less practical than our methods in scenarios with limited computational resources. We compare the efficiency of MBIB with MoE methods (RIDE and SADE) in Table 6.

5 Discussion

We have empirically observed a significant enhancement in network performance upon the introduction of BIB. Additionally, we undertook an exploration of two alternative mixture of BIB structures, as depicted in Figure 5. One structure applied sequential BIB connections between layer pairs (e.g., $BIB(v_1, v_2)$,

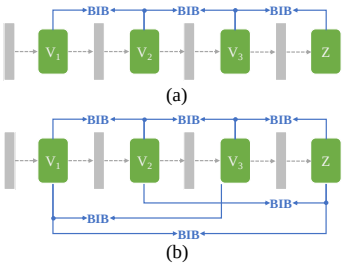

Figure 5: Two alternative multi-BIB structures.

$BIB(v_2, v_3)$, and $BIB(v_3, z)$), as shown in Figure 5(a), while the other integrated BIB connections among all feature representations as shown in Figure 5(b). We named them respectively as se-MBIB and all-MBIB. However, experiments on the CIFAR100-LT dataset have revealed that both se-MBIB and all-MBIB often exhibit worse performance compared to our MBIB method, as shown in Appendix F. The original intention to introduce sequential BIB connections was to propagate the optimal representation throughout the network in a cascading manner, where v_2 is considered a sufficient representation of v_1, v_3 is a sufficient representation of v_2, and z is a sufficient representation of v_3. This would ultimately result in z serving as a sufficient representation of v_1, consequently increasing the mutual information $I(z; y)$. However, this notion is inherently less rigorous, as even if v_2 is a sufficient representation of v_1 and v_3 is a sufficient representation of v_2, v_3 does not necessarily constitute a sufficient representation of v_1. While each individual BIB operation guarantees the output as an optimal and sufficient representation of the input, the sequential BIB connections do not inherently ensure that the global output is an optimal and sufficient representation of the initial input. In other words, the representation may deviate from the initial inputs and fall into local optima instead of global optima during the sequential propagation. Thus, se-MBIB with the sequential BIB connections appears to be less justifiable. The second structure all-MBIB, which introduces the improper sequential BIB connections on top of MBIB, is found to be detrimental to performance.

While our proposed methods demonstrate performance that falls slightly short of some state-of-the-art mixture of experts (MoE) models for long-tailed datasets, this presents a rich avenue for future research in BIB application. MoE methods involve the integration of multiple expert networks, each specialized in the recognition of distinct data segments. Our MBIB method could potentially be integrated into MoE frameworks. For example, MBIB may be incorporated into each expert network, enhancing the feature learning effectiveness of each expert, and thereby improving the overall performance. Inspired by two-stage methods, our network could explore staged training strategies, such as decoupling the training of the feature extractor and classifier, to optimize both components and ultimately achieve superior performance.

6 Conclusion

This paper proposes end-to-end learning methods named BIB and MBIB for long-tailed visual recognition from the perspective of information bottleneck. BIB uses self-distillation to implicitly optimize the objective and re-balance the classes to prevent poor performance in the optimization process due to the lack of tail class samples. Therefore, BIB can improve tail classes' performance without damaging head classes' performance. MBIB optimizes diverse information bottleneck within a single network simultaneously to utilize more information related to labels. Moreover, MBIB can fuse knowledge from different depths of the network to better fit the long-tailed data, further improving the model performance. Our experiments show that the quality of the feature spaces learned by BIB and MBIB is better than that of the re-balancing method like BSCE. We conducted experiments on commonly used long-tailed datasets, including CIFAR100-LT, ImageNet-LT, and iNaturalist 2018. The experimental results show that both BIB and MBIB perform well, even better than several recently proposed two-stage decoupling methods and MoE methods.

References

Alexander A. Alemi, Ian S. Fischer, Joshua V. Dillon, and Kevin P. Murphy. Deep variational information bottleneck. *ArXiv*, abs/1612.00410, 2017.

Shaden Alshammari, Yuxiong Wang, Deva Ramanan, and Shu Kong. Long-tailed recognition via weight balancing. In *CVPR*, 2022.

Shin Ando and Chun Yuan Huang. Deep over-sampling framework for classifying imbalanced data. In *Joint European Conference on Machine Learning and Knowledge Discovery in Databases*, pp. 770–785, 2017.

Mateusz Buda, Atsuto Maki, and Maciej A. Mazurowski. A systematic study of the class imbalance problem in convolutional neural networks. *Neural networks : the official journal of the International Neural Network Society*, 106:249–259, 2018.

Jonathon Byrd and Zachary Chase Lipton. What is the effect of importance weighting in deep learning? In *ICML*, 2019.

Kaidi Cao, Colin Wei, Adrien Gaidon, Nikos Aréchiga, and Tengyu Ma. Learning imbalanced datasets with label-distribution-aware margin loss. In *NeurIPS*, 2019.

Thomas M. Cover and Joy A. Thomas. Elements of information theory. 1991.

Jiequan Cui, Zhisheng Zhong, Shu Liu, Bei Yu, and Jiaya Jia. Parametric contrastive learning. In *Proceedings of the IEEE/CVF international conference on computer vision*, pp. 715–724, 2021.

Jiequan Cui, Shu Liu, Zhuotao Tian, Zhisheng Zhong, and Jiaya Jia. Reslt: Residual learning for long-tailed recognition. *IEEE Transactions on Pattern Analysis and Machine Intelligence*, 2022.

Yin Cui, Menglin Jia, Tsung-Yi Lin, Yang Song, and Serge J. Belongie. Class-balanced loss based on effective number of samples. *2019 IEEE/CVF Conference on Computer Vision and Pattern Recognition (CVPR)*, pp. 9260–9269, 2019.

Anirudh Goyal, Riashat Islam, Daniel Strouse, Zafarali Ahmed, Matthew M. Botvinick, H. Larochelle, Sergey Levine, and Yoshua Bengio. Infobot: Transfer and exploration via the information bottleneck. *ArXiv*, abs/1901.10902, 2019.

Boran Han. Wrapped cauchy distributed angular softmax for long-tailed visual recognition. In *Proceedings of the 40th International Conference on Machine Learning*, ICML'23, 2023.

Yin-Yin He, Jianxin Wu, and Xiu-Shen Wei. Distilling virtual examples for long-tailed recognition. In *Proceedings of the IEEE/CVF International Conference on Computer Vision (ICCV)*, pp. 235–244, October 2021.

Youngkyu Hong, Seungju Han, Kwanghee Choi, Seokjun Seo, Beomsu Kim, and Buru Chang. Disentangling label distribution for long-tailed visual recognition. *2021 IEEE/CVF Conference on Computer Vision and Pattern Recognition (CVPR)*, pp. 6622–6632, 2021.

Yan Jin, Mengke Li, Yang Lu, Yiu-ming Cheung, and Hanzi Wang. Long-tailed visual recognition via self-heterogeneous integration with knowledge excavation. In *Proceedings of the IEEE/CVF Conference on Computer Vision and Pattern Recognition*, pp. 23695–23704, 2023.

Bingyi Kang, Saining Xie, Marcus Rohrbach, Zhicheng Yan, Albert Gordo, Jiashi Feng, and Yannis Kalantidis. Decoupling representation and classifier for long-tailed recognition. In *International Conference on Learning Representations*, 2019.

Bingyi Kang, Yu Li, Sai Nan Xie, Zehuan Yuan, and Jiashi Feng. Exploring balanced feature spaces for representation learning. In *ICLR*, 2021.

Jaekyeom Kim, Minjung Kim, Dongyeon Woo, and Gunhee Kim. Drop-bottleneck: Learning discrete compressed representation for noise-robust exploration. *ArXiv*, abs/2103.12300, 2021.

Artemy Kolchinsky, Brendan D. Tracey, and David H. Wolpert. Nonlinear information bottleneck. *Entropy*, 21, 2019.

Thomas Laurent, James von Brecht, and Xavier Bresson. Long-tailed learning requires feature learning. In *The Eleventh International Conference on Learning Representations*, 2022.

Tianhong Li, Peng Cao, Yuan Yuan, Lijie Fan, Yuzhe Yang, Rogério Schmidt Feris, Piotr Indyk, and Dina Katabi. Targeted supervised contrastive learning for long-tailed recognition. 2021.

Tsung-Yi Lin, Priya Goyal, Ross B. Girshick, Kaiming He, and Piotr Dollár. Focal loss for dense object detection. *IEEE Transactions on Pattern Analysis and Machine Intelligence*, 42:318–327, 2020.

Hong Liu, Jeff Z. HaoChen, Adrien Gaidon, and Tengyu Ma. Self-supervised learning is more robust to dataset imbalance. *ArXiv*, abs/2110.05025, 2021.

Ziwei Liu, Zhongqi Miao, Xiaohang Zhan, Jiayun Wang, Boqing Gong, and Stella X. Yu. Large-scale long-tailed recognition in an open world. *2019 IEEE/CVF Conference on Computer Vision and Pattern Recognition (CVPR)*, pp. 2532–2541, 2019.

Yawei Luo, Ping Liu, Tao Guan, Junqing Yu, and Yi Yang. Significance-aware information bottleneck for domain adaptive semantic segmentation. *2019 IEEE/CVF International Conference on Computer Vision (ICCV)*, pp. 6777–6786, 2019.

Aditya Krishna Menon, Sadeep Jayasumana, Ankit Singh Rawat, Himanshu Jain, Andreas Veit, and Sanjiv Kumar. Long-tail learning via logit adjustment. *ArXiv*, abs/2007.07314, 2021.

Giung Nam, Sunguk Jang, and Juho Lee. Decoupled training for long-tailed classification with stochastic representations. *arXiv preprint arXiv:2304.09426*, 2023.

Gao Peifeng, Qianqian Xu, Peisong Wen, Zhiyong Yang, Huiyang Shao, and Qingming Huang. Feature directions matter: Long-tailed learning via rotated balanced representation. In *Proceedings of the 40th International Conference on Machine Learning*, pp. 27542–27563, 2023.

Jiawei Ren, Cunjun Yu, Xiao Ma, Haiyu Zhao, Shuai Yi, et al. Balanced meta-softmax for long-tailed visual recognition. *Advances in neural information processing systems*, 33:4175–4186, 2020.

Noam Slonim. The information bottleneck : Theory and applications. 2006.

Xudong Tian, Zhizhong Zhang, Shaohui Lin, Yanyun Qu, Yuan Xie, and Lizhuang Ma. Farewell to mutual information: Variational distillation for cross-modal person re-identification. *2021 IEEE/CVF Conference on Computer Vision and Pattern Recognition (CVPR)*, pp. 1522–1531, 2021.

N Tishby. The information bottleneck method. In *Proc. 37th Annual Allerton Conference on Communications, Control and Computing, 1999*, pp. 368–377, 1999.

Naftali Tishby and Noga Zaslavsky. Deep learning and the information bottleneck principle. *2015 IEEE Information Theory Workshop (ITW)*, pp. 1–5, 2015.

Laurens van der Maaten and Geoffrey E. Hinton. Visualizing data using t-sne. *Journal of Machine Learning Research*, 9:2579–2605, 2008.

Chaozheng Wang, Shuzheng Gao, Cuiyun Gao, Pengyun Wang, Wenjie Pei, Lujia Pan, and Zenglin Xu. Label-aware distribution calibration for long-tailed classification. *ArXiv*, abs/2111.04901, 2021a.

Jing Wang, Yuanjie Zheng, Jingqi Song, and Sujuan Hou. Cross-view representation learning for multi-view logo classification with information bottleneck. *Proceedings of the 29th ACM International Conference on Multimedia*, 2021b.

Wei Wang, Haojie Li, Zhengming Ding, F. Nie, Junyang Chen, Xiao Dong, and Zhihui Wang. Rethinking maximum mean discrepancy for visual domain adaptation. *IEEE Transactions on Neural Networks and Learning Systems*, 34:264–277, 2021c.

Xudong Wang, Long Lian, Zhongqi Miao, Ziwei Liu, and Stella X Yu. Long-tailed recognition by routing diverse distribution-aware experts. *arXiv preprint arXiv:2010.01809*, 2020.

Yidong Wang, Bowen Zhang, Wenxin Hou, Zhen Wu, Jindong Wang, and Takahiro Shinozaki. Margin calibration for long-tailed visual recognition. *ArXiv*, abs/2112.07225, 2021d.

Yuzhe Yang and Zhi Xu. Rethinking the value of labels for improving class-imbalanced learning. *ArXiv*, abs/2006.07529, 2020.

Han-Jia Ye, Hong-You Chen, De-Chuan Zhan, and Wei-Lun Chao. Identifying and compensating for feature deviation in imbalanced deep learning. *ArXiv*, abs/2001.01385, 2020.

Songyang Zhang, Zeming Li, Shipeng Yan, Xuming He, and Jian Sun. Distribution alignment: A unified framework for long-tail visual recognition. *2021 IEEE/CVF Conference on Computer Vision and Pattern Recognition (CVPR)*, pp. 2361–2370, 2021.

Yifan Zhang, Bryan Hooi, Lanqing Hong, and Jiashi Feng. Self-supervised aggregation of diverse experts for test-agnostic long-tailed recognition. In S. Koyejo, S. Mohamed, A. Agarwal, D. Belgrave, K. Cho, and A. Oh (eds.), *Advances in Neural Information Processing Systems*, volume 35, pp. 34077–34090. Curran Associates, Inc., 2022.

Yifan Zhang, Bingyi Kang, Bryan Hooi, Shuicheng Yan, and Jiashi Feng. Deep long-tailed learning: A survey. *IEEE Trans. Pattern Anal. Mach. Intell.*, 45(9):10795–10816, sep 2023.

Zhisheng Zhong, Jiequan Cui, Shu Liu, and Jiaya Jia. Improving calibration for long-tailed recognition. *2021 IEEE/CVF Conference on Computer Vision and Pattern Recognition (CVPR)*, pp. 16484–16493, 2021.

Zhisheng Zhong, Jiequan Cui, Eric Lo, Zeming Li, Jian Sun, and Jiaya Jia. Rebalanced siamese contrastive mining for long-tailed recognition. *ArXiv*, abs/2203.11506, 2022.

Boyan Zhou, Quan Cui, Xiu-Shen Wei, and Zhao-Min Chen. Bbn: Bilateral-branch network with cumulative learning for long-tailed visual recognition. *2020 IEEE/CVF Conference on Computer Vision and Pattern Recognition (CVPR)*, pp. 9716–9725, 2020a.

Boyan Zhou, Quan Cui, Xiu-Shen Wei, and Zhao-Min Chen. Bbn: Bilateral-branch network with cumulative learning for long-tailed visual recognition. In *Proceedings of the IEEE/CVF Conference on Computer Vision and Pattern Recognition (CVPR)*, June 2020b.

Zhipeng Zhou, Lanqing Li, Peilin Zhao, Pheng-Ann Heng, and Wei Gong. Class-conditional sharpness aware minimization for deep long-tailed learning. In *Proceedings of the IEEE/CVF Conference on Computer Vision and Pattern Recognition*, 2023.

A Proof of the Re-Balance Technique

According to VIB, $-I(v, y)$ and $-I(z, y)$ are bounded as $E_{p(v,y)} - \log q(y|v)$ and $E_{p(z,y)} - \log q(y|z)$. However, when the labels are long-tailed, we need to re-balance them. Our purpose is to train an end-to-end model, that is, the output of the model is $p_t(y|v)$. According to the properties of the conditional probability, we have

$$p_s(y_i|v)p_s(v) = p_s(v|y_i)p_s(y_i), \tag{18}$$

$$p_t(y_i|v)p_t(v) = p_t(v|y_i)p_t(y_i), \tag{19}$$

where the subscript s represents the training set distribution, and the subscript t represents the test set distribution. Since the training set and the testing set come from the same image domain, it can be assumed that $p_s(v) = p_t(v)$ and $p_s(v|y_i) = p_t(v|y_i)$. We have

$$\frac{p_s(y_i|v)}{p_s(y_i)} = \frac{p_t(y_i|v)}{p_t(y_i)}. \tag{20}$$

Due to $p_s(y_i) = \frac{n_i}{\sum_{j=1}^{K} n_j} = \frac{n_i}{N}$ and $p_t(y_i) = \frac{1}{K}$, we have $p_s(y_i|v) \propto n_i p_t(y_i|v)$. By normalizing $p_s(y_i|v)$, we get

$$p_s(y_i|v) = \frac{n_i p_t(y_i|v)}{\sum_{j=1}^{K} n_j p_t(y_j|v)}. \tag{21}$$

We can obtain $p_t(y_i|v)$ by the output of model, so that

$$p_t(y_i|v) \approx q_t(y_i|v) = \frac{e^{f_i(v;\theta)}}{\sum_{j=1}^{K} e^{f_j(v;\theta)}}. \tag{22}$$

We can rewrite Eq. (21) as

$$p_s(y_i|v) \approx q_s(y_i|v) = \frac{n_i e^{f_i(v;\theta)}}{\sum_{j=1}^{K} n_j e^{f_j(v;\theta)}}. \tag{23}$$

Therefore, we get the first loss as

$$Loss_1 = E_{p(v,y)} - \log q_s(y|v). \tag{24}$$

Similarly, for maximizing $I(z, y)$, we get the second loss as

$$Loss_2 = E_{p(z,y)} - \log q_s(y|z). \tag{25}$$

B Impact of different components of BIB

In order to further understand the influence of different components of the BIB loss function on the experimental results, we conducted ablation experiments on the loss function of BIB. As shown in Figure 6, when the β is not 0, the performance of the model can be improved, which indicates that information compression by information bottleneck is conducive to long-tailed visual recognition. On the other hand, if the use of $Loss_1$ and $Loss_2$ has not been re-balanced, even if the information bottleneck is used, it will not achieve satisfactory results.

Method	Balanced	$\beta = 0$
CE_2branch	✗	✓
SDIB	✗	✗
BSCE_2branch	✓	✓
BIB	✓	✗

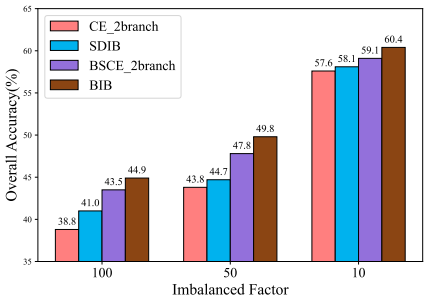

Figure 6: Ablation results of loss function. The Balanced option is ✗ means that the method uses cross entropy loss for $Loss_1$ and $Loss_2$. The β is 0 means that v and z are independent.

C Comparison between BIB and BSCE

From the form perspective, $Loss_1$ and $Loss_2$ are consistent with BSCE. In order to better understand our proposed BIB, we conducted extensive experiments on the ImageNet-LT with ResNet10. Table 7 shows the comparison results between BIB and BSCE. BSCE indicates that the network structure is the same as

branch v in BIB, and the loss function is BSCE. BSCE_MLP indicates that the network structure is the same as branch z in BIB, and the loss function is BSCE. BIB_v and BIB_z indicates the result obtained by directly using the output of $f(v;\theta)$ and $g(z;\theta)$. BIB_ensemble indicates the result obtained by the mean of $f(v;\theta)$ and $g(z;\theta)$, that is, the result we finally use. Table 7 shows that adding MLP only may hurt the performance of the model consistent with findings in Kang et al. (2019). Since IB can remove label-independent information from the representation as much as possible, the head classes performance of BIB_z has been significantly improved. At the same time, the tail classes performance has declined due to the limited number of tail class samples. However, the average performance has been greatly improved. We assume that v can retain all the information in x, but the information will still be lost from x to v. v is upstream of z in the information flow, and the improvement of the quality of z will also lead to the improvement of the quality of v, so the performance of BIB_v has also been greatly improved. At the same time, the mean of $f(v;\theta)$ and $g(z;\theta)$ can achieve the best performance.

Table 7: Comparison between BIB and BSCE on ImageNet-LT with ResNet10.

Method	Many	Medium	Few	All
BSCE	53.4	38.5	17.0	41.3
BSCE_MLP	51.7	36.6	18.2	39.9
BIB_v	53.8	**40.2**	**23.1**	43.1
BIB_z	54.6	38.5	19.2	42.1
BIB_ensemble	**54.7**	40.0	21.7	**43.2**

D Analysis of the Posterior Probability Distribution

From equation 14, we can infer that the closer the mean positive posterior probability of per class is to 1, the better. Figure 7 (a) shows the mean positive posterior probability $\overline{q}(y_i|x)$ of BIB. Figure 7 (b) presents the diff (diff= $\overline{q}_1(y_i|x) - \overline{q}_2(y_i|x)$) between the posterior probability obtained by BIB and CE. The results show that CE is severely over-fitting to the head class and under-fitting to the tail class. Figure 7 (c) presents the diff between the posterior probability obtained by BIB and BSCE, revealing BIB's superiority in most classes. (d) shows the mean positive posterior probability of MBIB. (e) presents the diff between the posterior probability obtained by MBIB and BIB, which shows that MBIB behaves better than BIB in the tail classes.

E Analysis of the Learned Representations Showed by t-SNE

We visualize the representation of the test set obtained by different models using t-SNE, as shown in Figure 8. The visualization results show that the separability of inter-class obtained by BIB and MBIB increases, and the representations within a class are more aggregated. Both quantitative analysis and visualization results show that the quality of representations obtained by BIB and MBIB are better than others. It indicates that BIB and MBIB get better classification performance, and the representation spaces become better simultaneously, which is consistent with our expectations.

F Experiments on Two Other Mixture of BIB Networks

We discussed two other Mixture of BIB network in the paper: one structure applied sequential BIB connections between layer pairs (se-MBIB), while the other integrated BIB connections among all feature representations (all-MBIB). In this section, we present the experiment results of the two alternative MBIB network. Figure 9 shows the performances of MBIB, se-MBIB and all-MBIB on CIFAR-100-LT (IF=100). It is evident that both se-MBIB and all-MBIB exhibit inferior performances compared to MBIB. The analysis can be found in the discussion section of the paper.

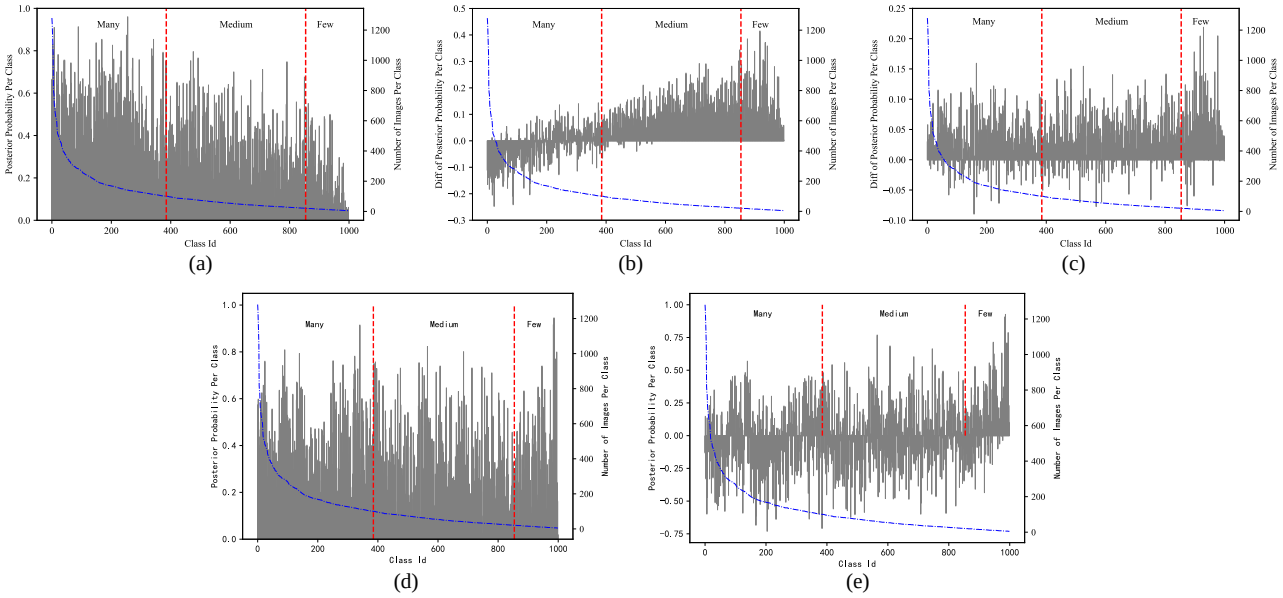

Figure 7: The mean Positive Posterior probability on ImageNet-LT with ResNet10. (a) The mean Positive Posterior probability per class of BIB. (b) Diff of the mean Positive Posterior probability per class between BIB and CE. (c) Diff of the mean Positive Posterior probability per class between BIB and BSCE.(d) The mean Positive Posterior probability per class of MBIB.(e) Diff of the mean Positive Posterior probability per class between MBIB and BIB.

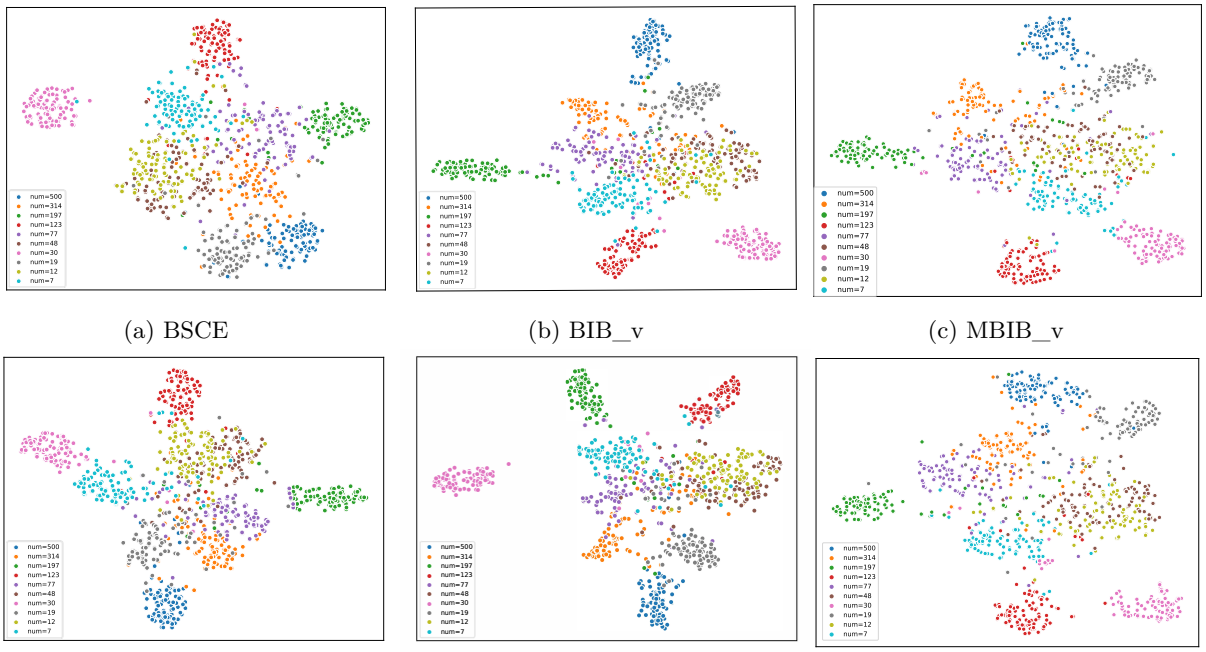

(a) BSCE (b) BIB_v (c) MBIB_v

(d) BSCE_MLP (e) BIB_z (f) MBIB_z

Figure 8: Visualization analysis. The t-SNE is used to visualize the test set feature space on CIFAR-100-LT (IF=100) and 10 classes are selected. The lower left corner shows the number of samples for each class during training.

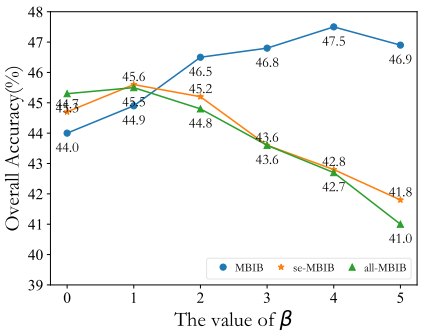

Figure 9: Overall accuracy of the three MBIB networks on CIFAR-100-LT (IF=100).